Journal of Hazardous Materials 382 (2020) 121015

Contents lists available at ScienceDirect

Journal of Hazardous Materials

journal homepage: www.elsevier.com/locate/jhazmat

Incorporation of strontium and calcium in geopolymer gels

Brant Walkley[a], Xinyuan Ke[a,b], Oday H. Hussein[a], Susan A. Bernal[a,c], John L. Provis[a,*]

[a] Department of Materials Science and Engineering, The University of Sheffield, Sheffield S1 3JD, UK
[b] Department of Architecture and Civil Engineering, University of Bath, Bath BA2 7AY, UK
[c] School of Civil Engineering, University of Leeds, Woodhouse Lane, Leeds LS2 9JT, UK

ARTICLE INFO

Editor: Daniel CW Tsang

Keywords:
Radionuclide encapsulation
Radioactive waste immobilisation
Geopolymers
Cementation

ABSTRACT

Radioactive waste streams containing ^{90}Sr, from nuclear power generation and environmental cleanup operations, are often immobilised in cements to limit radionuclide leaching. Due to poor compatibility of certain wastes with Portland cement, alternatives such as alkali aluminosilicate 'geopolymers' are being investigated. Here, we show that the disordered geopolymers ((N,K)-A-S-H gels) formed by alkali-activation of metakaolin can readily accommodate the alkaline earth cations Sr^{2+} and Ca^{2+} into their aluminosilicate framework structure. The main reaction product identified in gels cured at both 20 °C and 80 °C is a fully polymerised Al-rich (N,K)-A-S-H gel comprising Al and Si in tetrahedral coordination, with Si in $Q^4(4Al)$ and $Q^4(3Al)$ sites, and Na^+ and K^+ balancing the negative charge resulting from Al^{3+} in tetrahedral coordination. Faujasite-Na and partially Sr-substituted zeolite Na-A form within the gels cured at 80 °C. Incorporation of Sr^{2+} or Ca^{2+} displaces some Na^+ and K^+ from the charge-balancing sites, with a slight decrease in the Si/Al ratio of the (N,K)-A-S-H gel. Ca^{2+} and Sr^{2+} induce essentially the same structural changes in the gels. This is important for understanding the mechanism of incorporation of Sr^{2+} and Ca^{2+} in geopolymer cements, and suggests that geopolymer gels are excellent candidates for immobilisation of radioactive waste containing ^{90}Sr.

1. Introduction

Conditioning of radioactive waste arising from nuclear facility operation and decommissioning is essential to its safe disposal and environmental remediation. Cementation offers significant advantages over other waste conditioning routes (such as thermal conversion of ceramics or glasses) including simplicity, relatively high throughput, low cost, and the absence of secondary waste generation (Aldridge et al., 1997). Immobilisation of radionuclides such as strontium-90 (^{90}Sr, $T_{1/2}$ = 28.80 yrs) by cementation has received particular attention due to its presence as a fission product, including in nuclear reactor cooling water (Qian et al., 2002; Ochs et al., 2015; Kuenzel et al., 2015), which necessitates the use of granular ion exchange resins which must then be conditioned prior to disposal (Tusa, 2014). Traditionally, strontium-containing waste has been encapsulated in Portland cement (PC), which has shown potential for uptake of Sr as well as lanthanides and actinides including Nd, U, and Np. Sr uptake is usually via sorption to the surface of calcium silicate hydrate (C-S-H) (Tits et al., 2015; Vespa et al., 2014; Gaona et al., 2012; Mandaliev et al., 2010; Wieland et al., 2008; Tits et al., 2006), but co-precipitation of the strontium silicate hydrate phase $Sr_5Si_6O_{16}(OH)_2.5H_2O$ exhibiting structural similarity to tobermorite ($Ca_5Si_6O_{16}(OH)_2.xH_2O$, where x = 4 or 5) has been observed (Felmy et al., 2003). Furthermore, C-S-H is space-filling and hence restricts ion mobility. However, the high water content of PC and the prevalence of hydrate phases means that the mechanism of Sr^{2+} uptake involves adsorption to partially hydrated phases such as calcium silicate hydrate through reversible ion-exchange interactions (Wieland et al., 2008; Tits et al., 2006), while retention of other radioisotopes such as Cs may be too low to prevent diffusion into the environment (Goñi et al., 2006). Consequently, the applicability of encapsulation of these radionuclides in PC is limited.

Alkali aluminosilicate cements, often called geopolymers, comprise a fully polymerised, three-dimensionally cross-linked, structurally disordered alkali aluminosilicate network. Because of their cation-binding sites, mechanical properties and chemical resistance, these materials have received significant interest in recent years as suitable materials for the cementation of radioactive waste (Arbel Haddad et al., 2017; Williams et al., 2016; Provis et al., 2008; Ofer-Rozovsky et al., 2019). The alkali aluminosilicate hydrate gel framework is often abbreviated as (N,K)-A-S-H, as Na and K are the most common alkalis used in their production, and it has a pseudo-zeolitic or proto-zeolitic structure (Provis et al., 2015). Al and Si are both present in tetrahedral coordination, analogous to their roles in zeolites, with Si existing in $Q^4(m\text{Al})$ environments ($1 \leq m \leq 4$ depending on the Al/Si ratio of the

* Corresponding author.
E-mail address: j.provis@sheffield.ac.uk (J.L. Provis).

https://doi.org/10.1016/j.jhazmat.2019.121015
Received 27 June 2019; Received in revised form 8 August 2019; Accepted 13 August 2019
Available online 17 August 2019

gel), while Al is predominantly in $q^4(4Si)$ environments because of the energetic penalty associated with $Al^{IV}-O-Al^{IV}$ bonding (Provis et al., 2005a). The negative charge associated with Al substitution for Si is balanced by the alkali cations. The gel nanostructure can be significantly affected by kinetic limitations on silica and alumina release from solid precursors used in gel synthesis (Hajimohammadi et al., 2010, 2011) and it consequently evolves as the alkali activation reaction proceeds.

Due to the pseudo-zeolitic gel nanostructure, crystalline zeolite phases with longer-range order have been observed to form in geopolymer gels when held at elevated temperatures (Rivera et al., 2016; Rickard et al., 2015, 2011). The temperature-dependent phase stability of geopolymer gel-based wasteforms is of particular importance, as wasteforms which are stored in geological disposal facilities are expected to experience temperatures of 20 °C during initial storage above ground (Hunter and Swift, 2013; Godfrey and Cann, 2015; Boden, 2002; Nuclear Decommissioning Authority, 2014) and between 35 °C and 80 °C across the first 100 years of their storage in the geological disposal facility (Boden, 2002; Nuclear Decommissioning Authority, 2014; Prentice et al., 2019).

Previous work utilising high resolution transmission electron microscopy coupled with energy dispersive X-ray spectroscopy and selected area electron diffraction has identified incorporation of 1–2 mol. % Sr in amorphous geopolymer gels with molar Si/Al = 2.0 and Na/Al = 1 (Blackford et al., 2007; Perera et al., 2006). The gels were loaded with 5 wt. % Sr during formulation, with the remaining Sr preferentially forming $SrCO_3$ rather than being incorporated into the geopolymer gel. Synthetic (calcium, alkali) aluminosilicate gels loaded with 0.1 wt. % Sr showed retention of up to 99.9% Sr^{2+} when leaching for 7 days at 20 °C in MilliQ water, with Sr retention enhanced by reduction of the Si/Al and Ca/(Si + Al) (independently of Si/Al) molar ratios in the (calcium, alkali) aluminosilicate gels (Vandevenne et al., 2018). This was attributed to increased formation of N-A-S-H, relative to the predominant sodium- and aluminium-substituted calcium silicate hydrate gel, for gels with lower Ca/(Si + Al) molar ratios. Together, these findings demonstrate the potential for geopolymer cements to yield suitable wasteforms for the cementation of radioactive waste.

Despite these recent advances, and the interest in immobilisation of radionuclides within non-Portland cements, the transport, solubility and incorporation processes which control the long-term performance of these wasteforms are still not well understood. In particular, a detailed analysis and understanding of the incorporation of Sr (either as ^{90}Sr or the non-radioactive isotopes of Sr) in geopolymer gels at the atomic scale is not yet available.

Here, we investigate the mechanism of incorporation of non-radioactive isotopes of Sr^{2+} and Ca^{2+} in a series of metakaolin-based geopolymer gels, to assess their potential as materials for cementation of radioactive waste. Ca^{2+} was also investigated to compare the effects of the differing ionic radii of these two divalent cations (Shannon radii r = 1.18 Å and 1.00 Å for Sr^{2+} and Ca^{2+}, respectively) (Shannon, 1976). The trace element level radionuclide loading investigated is representative of that expected for wasteforms produced by cementation of radioactive ion exchange resins (Kirishima et al., 2015; Koma et al., 2017). Multinuclear magic angle spinning (MAS) and cross polarisation (CP) MAS nuclear magnetic resonance (NMR) spectroscopy probing the local environments of ^{29}Si, ^{27}Al and ^{23}Na, in conjunction with Fourier transform infrared (FTIR) spectroscopy and X-ray diffraction (XRD) measurements, are used to examine any nanostructural changes that may be induced by incorporation of the alkaline earth cations, and to investigate the influence of the alkali cations Na^+ and K^+ on the incorporation mechanism of the alkaline earth cations. The findings presented here have significant implications for the long term stability and durability of these materials and suggest that metakaolin-based geopolymer gels are attractive candidate wasteforms for immobilisation of radioactive waste containing radioactive ^{90}Sr.

Table 1
Metakaolin chemical composition (wt.%) as determined by X-ray fluorescence analysis (LOI: loss on ignition at 1000 °C).

Na_2O	Al_2O_3	SiO_2	P_2O_5	K_2O	CaO	TiO_2	Fe_2O_3	SrO	LOI
0.3	44.4	52.6	0.1	0.2	< 0.05	1.0	0.6	< 0.05	0.8

2. Experimental methods

2.1. Sample preparation

Geopolymer gels were produced by reaction of metakaolin (MetaStar 501, Imerys, composition as determined by X-ray fluorescence provided in Table 1, D_{50} = 4.57 μm) with a sodium silicate, potassium silicate, or mixed alkali (containing both sodium and potassium silicate) activating solution.

The activating solutions were prepared by dissolving sodium hydroxide powder (AnalaR 99 wt.%), potassium hydroxide powder (AnalaR 99 wt.%), or a combination of both, in sodium silicate (PQ-NS, 44.1 wt.% sodium silicate, with a solution modulus of SiO_2/M_2O = 2.1, with the balance water, PQ UK) or potassium silicate solution (PQ-KS, 51.6 wt.% potassium silicate, with a solution modulus of SiO_2/M_2O = 2.2, with the balance water, PQ UK) and distilled water. Stoichiometry was designed to obtain an activating solution modulus of SiO_2/M_2O = 1 (where M represents Na and/or K), an activator dose such that M_2O/Al_2O_3 = 1 and SiO_2/Al_2O_3 = 3 (Si/Al = 1.5) in the final reaction mixture, water content such that M_2O/H_2O = 11, and the nominal chemical composition and water/solids (w/s) ratios outlined in Table 2.

The activating solution was mixed with metakaolin to form a homogeneous paste which was subsequently cast in sealed containers cured for 3 months at either 20 °C ± 2 °C or 80 °C ± 2 °C. Reactant proportions were approximately 40 wt. % metakaolin, 44 wt. % alkaline activating solution and 16 wt. % additional water. Samples containing nominally natural abundance proportions of the isotopes of alkaline earth cations Ca^{2+} and Sr^{2+} were produced by mixing metakaolin, the activating solution (prepared as described above) and either $Ca(OH)_2$ (Sigma Aldrich) or $Sr(OH)_2{\cdot}8H_2O$ (Sigma Aldrich) to obtain ME/Al = 0.00025 (where ME represents the alkali earth cations Sr^{2+} or Ca^{2+}) in the final reaction mixture. This concentration is representative of that expected for wasteforms produced by cementation of radioactive ion exchange resins (Kirishima et al., 2015; Koma et al., 2017).

2.2. Characterisation

The hardened binders were hand ground using a pestle and mortar, immersed in acetone for 15 min to remove loosely bound water (thereby halting the alkali-activation reaction without significantly altering the geopolymer gel structure (Ismail et al., 2013)), and subsequently filtered prior to storing in a sealed desiccator under vacuum.

Table 2
Nominal chemical composition (molar basis) of the alkali activating solution.

		Mole fraction				
Sample	Code	Na_2O	K_2O	Sr/Al	Ca/Al	w/s
A	Na	1.0	0.0	0	0	0.4
B	Na.K	0.5	0.5	0	0	0.4
C	K	0.0	1.0	0	0	0.4
D	Na-Sr	1.0	0.0	0.00025	0	0.4
E	Na.K-Sr	0.5	0.5	0.00025	0	0.4
F	K-Sr	0.0	1.0	0.00025	0	0.4
G	Na-Ca	1.0	0.0	0	0.00025	0.4
H	Na.K-Ca	0.5	0.5	0	0.00025	0.4
I	K-Ca	0.0	1.0	0	0.00025	0.4

2.2.1. X-ray diffraction

X-ray diffraction (XRD) data were obtained to examine the long-range ordering and crystallinity of the reaction products in each sample. Data were obtained across a 2θ range of 5°-70° using a Panalytical X'Pert^3 Powder X-ray diffractometer with Cu Kα radiation (1.54 Å), a nickel filter, a step size of 0.020° and a count time of 1 s/step. Diffracted background intensity at low angles was reduced using an anti-scatter blade, and an incident beam divergence of 1.0 mm and a 2.5 ° Soller slit in the diffracted beam were used. Phase identification was performed using Diffrac.EVA V4.1 software with the ICDD PDF4 + 2015 database.

2.2.2. Solid state nuclear magnetic resonance spectroscopy

Solid state single pulse ^{29}Si, ^{27}Al and ^{23}Na magic angle spinning (MAS) NMR data were obtained to examine the local structure of the reaction products in each sample. All spectra were acquired on a Bruker Avance III HD 500 spectrometer at 11.7 T (B_0) using a 4.0 mm dual resonance CP/MAS probe, yielding a Larmor frequency of 99.35 MHz for ^{29}Si, 130.32 MHz for ^{27}Al and 132.29 MHz for ^{23}Na. ^{29}Si MAS NMR spectra were acquired using a 5.5 µs non-selective (π/2) excitation pulse, a measured 90 s relaxation delay, a total of 256 scans and spinning at 12.5 kHz. ^{1}H-^{29}Si cross-polarisation (CP) MAS NMR experiments were performed using the same instrument with a spinning frequency of 12.5 kHz, a ^{29}Si non-selective (π/2) pulse width of 1.7 µs, an initial ^{1}H non-selective (π/2) pulse width of 2.5 µs, a recycle delay of 1.5 s and Hartmann-Hahn contact periods of 1.7 ms. A nominal ^{1}H decoupling field strength of 80 kHz was employed during acquisition and 10,240 scans were collected per experiment. ^{27}Al MAS NMR spectra were acquired using a 1.7 µs non-selective (π/2) excitation pulse, a measured 10 s relaxation delay, a total of 128 scans and spinning at 12.5 kHz. ^{23}Na MAS NMR spectra were acquired using a 3 µs non-selective (π/2) excitation pulse, a measured 10 s relaxation delay, a total of 128 scans and spinning at 12.5 kHz. All ^{29}Si, ^{27}Al and ^{23}Na spectra were referenced to pure tetramethylsilane (TMS), 1.0 M aqueous $Al(NO_3)_3$ and 1.0 M aqueous $NaCl_{(aq)}$, respectively, at 0 ppm.

Gaussian peak profiles were used to deconvolute the ^{29}Si MAS and ^{1}H-^{29}Si CPMAS NMR spectra (Massiot et al., 2002). The minimum number of peaks possible were fitted, and the isotropic chemical shift (δ_{iso}) and peak full width at half maximum (FWHM) of each resonance were required to be consistent in both the ^{29}Si MAS NMR and ^{1}H-^{29}Si CP MAS NMR spectral deconvolutions. Peak intensities were required to be consistent with the structural constraints described by the thermodynamics of a statistical distribution of Si and Al sites within a Q^4 aluminosilicate network for (N,K)-A-S-H gel products (Provis et al., 2005a). Previous work utilising ^{29}Si and ^{27}Al MAS NMR and Fourier transform infrared spectroscopy has shown that these models best describe the environments in which Si and Al exist in (N,K)-A-S-H gels (Provis et al., 2005a; Fernández-Jiménez et al., 2006; Lecomte et al., 2006; Criado et al., 2008; Walkley et al., 2016). In all spectral deconvolutions congruent dissolution was assumed, and the contribution from unreacted precursor particles was taken into account by fitting a scaled component spectrum calculated from the ^{29}Si and ^{27}Al MAS NMR spectrum of unreacted metakaolin.

2.2.3. Fourier transform infrared spectroscopy

Fourier transform infrared (FTIR) spectroscopy data were obtained to examine the local structure of the reaction products in each sample. Samples for FTIR spectroscopy analysis were prepared by mixing 2 mg of sample with 200 mg KBr and pressing the mixture into a pellet. FTIR spectra were measured using a Perkin Elmer Frontier Mid FT-IR spectrometer equipped with a deuterated triglycine sulfate (DTGS) detector and KBr beam splitter optical system, scanning 16 times at a resolution of 4 cm^{-1}.

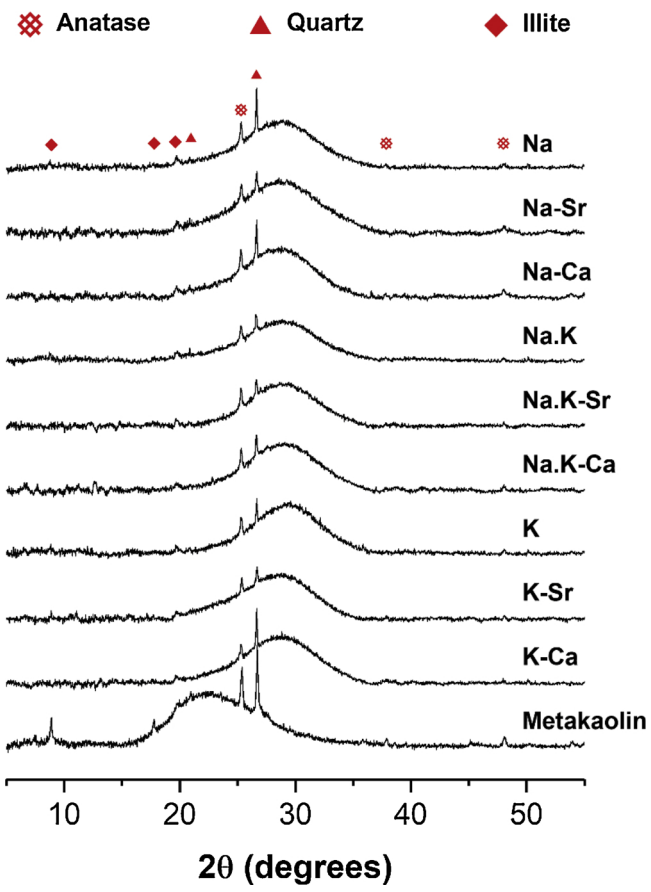

Fig. 1. X-ray diffraction data for unreacted metakaolin and the geopolymer gels cured at 20 °C, as a function of the activator and radionuclide simulant type.

3. Results and discussion

3.1. X-ray diffraction

XRD data for unreacted metakaolin and for each geopolymer gel cured at 20 °C are shown in Fig. 1. Data for unreacted metakaolin displays a dominant broad feature due to diffuse scattering centred at approximately 22° 2θ, consistent with its amorphous nature. Reflections due to the crystalline phases anatase (TiO_2, Powder Diffraction File (PDF) # 01-084-1286), quartz (SiO_2, PDF # 01-078-2315) and hydroxylated muscovite (illite-2, $(K,H_3O)(Al,Mg,Fe)_2(Si,Al)_4O_{10}[(OH)_2, (H_2O)]$, PDF # 00-026-0911) are observed in the X-ray diffraction pattern for unreacted metakaolin. The X-ray diffraction patterns for each geopolymer gel cured at 20 °C exhibit a dominant broad feature due to diffuse scattering, centred at approximately 29° 2θ, and indicating the formation of a crystallographically disordered reaction product (Duxson et al., 2006; Provis et al., 2005b). Reflections assigned to anatase, quartz and hydroxylated muscovite are also visible in the XRD data for each aluminosilicate gel and indicate that while these phases remain largely intact throughout the reaction process under these conditions, small changes in the intensity of the reflections assigned to hydroxylated muscovite suggest partial reaction and/or changes in crystallinity due to partial reaction of hydroxylated muscovite has occurred. A small amount of unreacted metakaolin is also observed by solid state NMR in all geopolymer gel samples, and is discussed further below.

The X-ray diffraction patterns for each geopolymer gel cured at 80 °C (Fig. 2) also exhibit a dominant broad feature due to diffuse scattering from (N,K)-A-S-H gel centred at approximately 29° 2θ, as at 20 °C, and the peaks assigned to anatase, quartz and hydroxylated

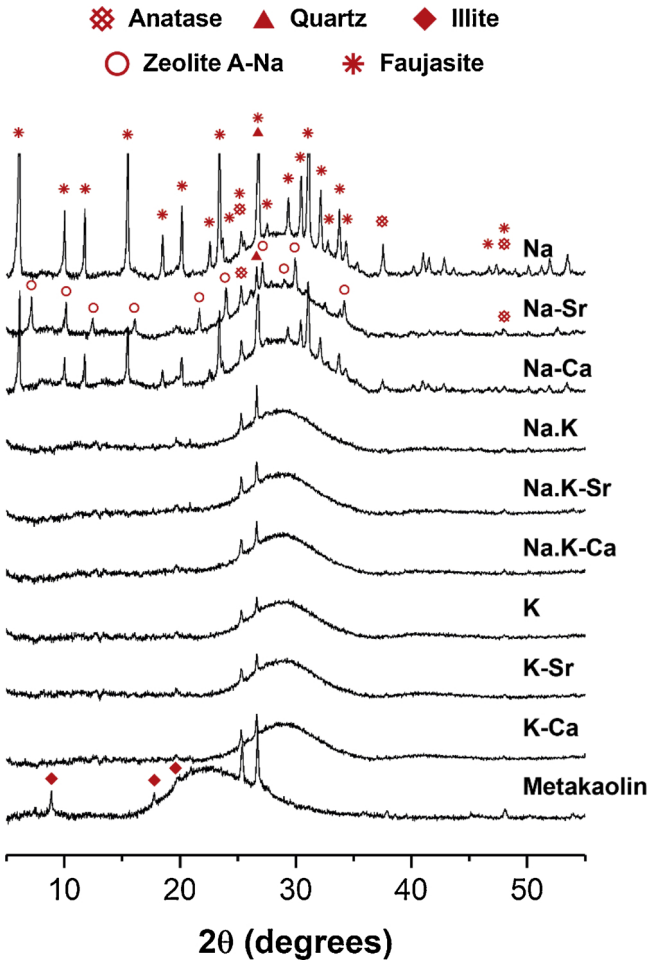

Fig. 2. X-ray diffraction data for unreacted metakaolin and the geopolymer gels cured at 80 °C, as a function of the activator and radionuclide simulant type.

muscovite are again observed. The XRD data for geopolymer gels produced by reaction of metakaolin with potassium silicate, or with a combination of sodium silicate and potassium silicate, do not exhibit any other observable reflections of crystalline phases. No differences observable by XRD are induced by the presence of alkaline earth cations at the concentrations used here.

The X-ray diffraction patterns for the geopolymer produced by reaction of metakaolin with sodium silicate at 80 °C exhibit, in addition to those identified above, reflections due to the zeolite faujasite-Na ($Na_7[Al_7Si_{17}O_{48}]\cdot 32(H_2O)$, PDF 48-0731). The formation of crystalline zeolite phases from the geopolymer gels cured at 80 °C is consistent with the proto-zeolitic structure that has been identified in alkali aluminosilicate gels synthesised directly under similar conditions (Provis et al., 2005b). Hydrothermal synthesis of faujasite-Na at 80 °C has been previously reported to be favourable at Si/Al ratios close to unity in the presence of Na^+ cations (Barrer and Mainwaring, 1972a; Davis and Lobo, 1992). In the presence of K^+ (either in Na^+-free or mixed alkali systems containing both Na^+ and K^+) formation of chabazite-K is favoured when $2 \leq Si/Al \leq 4.5$, and faujasite formation has not been previously observed (Barrer and Mainwaring, 1972a; Barrer et al., 1968; Barrer and Mainwaring, 1972b). Furthermore, previous work has shown that small alkali metal cations produce the highest rates of zeolite nucleation (McCormick and Bell, 1989), and chabazite-type zeolite crystallite yield decreases with increasing K^+ (in the form of KOH) concentration (Barrer and Mainwaring, 1972b). Geopolymers produced by alkali-activation of fly ash with potassium silicate also display a lower extent of crystallisation than those produced by alkali-activation of fly ash with sodium silicate (van Jaarsveld and van Deventer, 1999). Together, these previous observations are consistent with the formation of faujasite-Na in the geopolymer cement produced by reaction of metakaolin with sodium silicate at 80 °C, and the absence of any zeolite phases in the geopolymer cements produced by reaction of metakaolin with potassium silicate or a mixture of sodium and potassium silicate at 80 °C (where $Si/Al < 2$).

The presence of a low content of Ca^{2+} (r = 1.00 Å) does not alter the nature of the reaction products formed due to its similarity in size with Na^+ (r = 1.02 Å), however the intensity of the reflections due to crystalline phases is decreased, suggesting a lower extent of formation of these phases. Suppression of zeolite crystallisation in the presence of Ca^{2+} has been previously observed, including in geopolymers (Provis et al., 2005b; Catalfamo et al., 1997; Phair et al., 2003). This results from the larger number of potential nucleation sites and therefore smaller mean crystallite size, as well as from the reduction in Si supersaturation levels due to formation of calcium silicate hydrates (Catalfamo et al., 1997; Jacobs, 1992). The presence of Sr^{2+} (r = 1.18 Å) in the geopolymer gel produced by reaction of metakaolin with sodium silicate results in formation of a zeolite A-type phase, the structure of which may contain some Sr although there is not sufficient change in lattice parameter to enable us to distinguish between the LTA structures of both zeolite A-Na ($Na_{12}[(AlO_2)_{12}(SiO_2)_{12}]\cdot 27H_2O$, PDF # 39-0222) and a partially Sr-substituted zeolite A-Na ($(Na,Sr)_{12}[(AlO_2)_{12}(SiO_2)_{12}]\cdot 27H_2O$, PDF # 38-0243). Previous work has shown strong adsorption selectivity for Sr^{2+} in zeolite A (when compared with faujasite-Na) in the presence of Na^+ and K^+ due to the high cation exchange capacity of the LTA structure (Munthali et al., 2015), aligning with the observation of reflections due to zeolite A in the XRD data for geopolymer cements produced by reaction of metakaolin with sodium silicate at 80 °C and in the presence of Sr. The extent of formation of zeolite A is much lower than that of faujasite-Na formed in the Sr^{2+}-free geopolymers produced by alkali-activation of metakaolin with sodium silicate. This is consistent with the larger ionic radius of Sr^{2+} (r = 1.18 Å) compared with Na^+ (r = 1.02 Å), which results in a decrease in zeolite nucleation and formation (McCormick and Bell, 1989).

3.2. Solid state nuclear magnetic resonance spectroscopy

3.2.1. ^{29}Si MAS and ^{1}H-^{29}Si CP MAS NMR

The ^{29}Si MAS and ^{1}H-^{29}Si CP MAS NMR spectra for unreacted metakaolin and the geopolymer gels cured at 20 °C are shown in Fig. 3. ^{29}Si MAS NMR data for unreacted metakaolin exhibits a single broad resonance at δ_{iso} between -80 to -125 ppm with maximum intensity at δ_{iso} = -107 ppm. This indicates an extensive distribution of Si environments and chemical shifts, consistent with the broad amorphous feature observed in the XRD data for unreacted metakaolin and with previous ^{29}Si MAS NMR observations for similar materials (Duxson et al., 2005a). This resonance contains contributions from a distribution of $Q^4(mAl)$ environments (where $0 \leq m \leq 4$), with the maximum intensity at δ_{iso} = -107 ppm indicating that this distribution is dominated by species with lower Al substitution ($Q^4(0Al)$ and $Q^4(1Al)$ sites). Quartz (identified by XRD, Fig. 1) will also contribute to the ^{29}Si MAS NMR spectrum of metakaolin at approximately δ_{iso} = -110 (± 3) ppm due to resonance of $Q^4(0Al)$ sites (Kowalczyk and Roberts, 1994; Myers et al., 1998; Bernal et al., 2013), however due to the very long ^{29}Si relaxation times (on the order of 1 h) (Kowalczyk and Roberts, 1994; Myers et al., 1998) and the extensive disorder of Si sites in metakaolin, the $Q^4(0Al)$ site in quartz cannot be resolved unambiguously in the spectra presented here. ^{29}Si MAS NMR data for illite exhibit resonances within the region δ_{iso} = -85 to -95 ppm, (Lausen et al., 1999) and therefore this phase also contributes to the signal in this region in the spectra presented here.

The ^{29}Si MAS NMR spectra of the geopolymer gels each exhibit a broad resonance spanning from δ_{iso} = -75 to -110 ppm and centred at δ_{iso} = -87.8 ppm, with a consistent lineshape of the distribution of δ_{iso} across all samples. This resonance is attributed to a distribution of

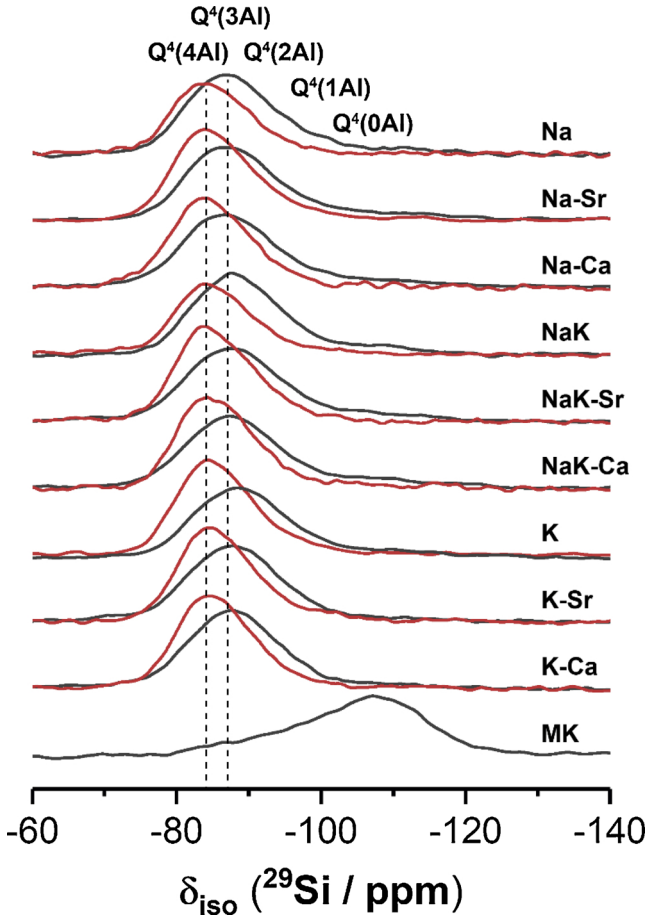

Fig. 3. ^{29}Si MAS (B_0 = 11.7 T, ν_R = 12.5 kHz, shown in black) NMR and ^{1}H-^{29}Si CPMAS (B_0 = 11.7 T, ν_R = 12.5 kHz and Hartmann-Hahn contact period t = 1.7 ms, shown in red) NMR spectra for each geopolymer gel and for metakaolin. (For interpretation of the references to colour in this figure legend, the reader is referred to the web version of this article).

$Q^4(m\text{Al})$ environments within a (N,K)-A-S-H gel (Walkley et al., 2016; Duxson et al., 2005b), and the shift in the resonance compared with that of metakaolin indicates that alkali activation of metakaolin has resulted in formation of a reaction product dominated by higher Al substituted Q^4(4Al) and Q^4(3Al) sites.

The ^{1}H-^{29}Si CP MAS NMR spectra of the geopolymer gels each exhibit a broad resonance spanning from δ_{iso} = -75 to -95 ppm and centred at δ_{iso} = -83.8 ppm, again with a consistent lineshape of the distribution of δ_{iso} across all samples. The ^{1}H-^{29}Si CP MAS NMR signal is sensitive to the internuclear distance between the Si atoms and nearby protons, such that ^{1}H-^{29}Si CP MAS NMR signal of Si atoms in closest proximity to protons is preferentially enhanced (Kolodziejski and Klinowski, 2002) and this data therefore indicates those Si species within the hydrated reaction product. Consequently, it is possible to differentiate between resonances resulting from hydrated Si species in the (N,K)-A-S-H gel and unreacted Si species in remnant unreacted metakaolin particles. The maximum intensity at δ_{iso} = -83.8 ppm in the ^{1}H-^{29}Si CP MAS NMR spectra of the geopolymer gels indicates that the hydrated (N,K)-A-S-H gel contains primarily Q^4(4Al) Si sites, independent of the activator used.

Deconvolution and quantification of the ^{29}Si MAS and ^{1}H-^{29}Si CPMAS NMR data (Fig. 4 and Table 3) identify the presence of two new Si environments which form in each geopolymer gel upon alkali activation of metakaolin. These environments resonate at δ_{iso} = -84.7 and -89.0 ppm, respectively, and are attributed to Q^4(4Al) and Q^4(3Al) sites within a fully polymerised, Al-rich (Si/Al ≤ 1.2) (N,K)-A-S-H gel (Provis et al., 2005a). The molar Si/Al ratio of the (N,K)-A-S-H gel may be calculated using Engelhardt's formula (Engelhardt et al., 1981) (Eq. 1):

$$\frac{\text{Si}}{\text{Al}} = \frac{\sum_{m=1}^{4} I_{AQ^4(m\text{Al})}}{\sum_{m=1}^{4} 0.25 \times m \times I_{AQ^4(m\text{Al})}} \quad (1)$$

where $I_{AQ^4_{(m\text{Al})}}$ refers to the normalised relative integral areas of the resonances in the ^{29}Si MAS NMR spectral deconvolutions of each $Q^4(m\text{Al})$ site within the (N,K)-A-S-H gel (i.e. excluding resonances due to $Q^4(m\text{Al})$ sites within remnant unreacted metakaolin).

Eq. 1 requires that Loewenstein's rule is obeyed such that there are negligible Al-O-Al bonds present. This assumption has been shown to be valid by application of ^{17}O 3QMAS NMR spectroscopy to synthetic geopolymer gels with Si/Al > 1 (Walkley et al., 2018), and can therefore be safely assumed here where the nominal Si/Al = 1.5 for each geopolymer gel. Each (N,K)-A-S-H gel exhibits a Si/Al = 1.20 to 1.26. This value is lower than that of the initial reaction mixtures, indicating preferential precipitation of an Al-rich gel. Incorporation of alkaline earth cations Ca^{2+} and Sr^{2+} results in a slight increase in Q^4(4Al) sites and a slight decrease in Q^4(3Al) sites (Table 3), and consequently a slight decrease in the Si/Al ratio of the (N,K)-A-S-H gel (Table 3). This is likely to be due to the increased charge balancing capacity resulting from substitution of a divalent charge alkaline earth cation for a monovalent alkali cation. The magnitude of the decrease in Si/Al ratio of the gel appears to be influenced by the alkali cations present, with K^+ resulting in a greater increase in the Si/Al ratio of the gel, compared with Na^+, upon incorporation of Ca^{2+} or Sr^{2+}. There is no variation (within the estimated error) in the Si/Al ratio of the geopolymer gels when comparing between the incorporation of Ca^{2+} or Sr^{2+}, indicating that both alkaline earth cations induce comparable structural changes.

3.2.2. ^{27}Al MAS NMR

The ^{27}Al MAS NMR spectrum for unreacted metakaolin (Fig. 5) displays three broad resonances exhibiting distributions of δ_{obs} (observed chemical shift) with maximum intensity at δ_{obs} = 56, 33 and 8 ppm, respectively, attributed to Al in tetrahedral, pentahedral and octahedral coordination (Duxson et al., 2005c; Kobera et al., 2014).

The ^{27}Al MAS NMR spectrum for each geopolymer gel cured at 20 °C exhibits a broad tetrahedral Al resonance spanning from δ_{obs} = 70 to 50 ppm and centred at δ_{obs} = 60.7 ppm. This resonance is attributed to Al within a full polymerised tetrahedral (q^4) site in a (N,K)-A-S-H type gel (Walkley et al., 2018; Duxson et al., 2005c), with the negative charge arising from the substitution of Al^{3+} for Si^{4+} balanced by alkali cations (Na^+ or K^+). The presence of Al in exclusively tetrahedral coordination is expected due to the presence of excess alkali cations (Stebbins et al., 2000) and indicates that all Al within metakaolin has reacted, consistent with the ^{29}Si MAS and ^{1}H-^{29}Si CPMAS NMR observations of preferential dissolution of Al during alkali activation discussed above. The lineshape and width of the distribution of δ_{obs} for this resonance are identical across all samples, regardless of the presence of, or variation in, different alkali (Na^+ or K^+) or alkaline earth (Ca^{2+}, Sr^{2+}) cations. Slight shielding of the ^{27}Al nuclei is observed when K^+ is present, resulting in δ_{obs} = 60.9 ppm for geopolymer gels activated with sodium silicate compared with δ_{obs} = 60.6 ppm for geopolymer gels activated with potassium silicate or a combination of sodium and potassium silicates. This is consistent with the presence of a larger transverse magnetic field within the local environment surrounding the Al atoms, induced by replacement of some of the charge balancing Na^+ ions within the first coordination sphere of Al^{3+} with larger charge balancing K^+ ions. A slight narrowing of the distribution of δ_{obs} and an increase in intensity (between 1 and 3%) of the maximum of this distribution with addition of Sr^{2+} and Ca^{2+} is observed for all samples, consistent with the slight reduction in the Al/Si ratio observed by ^{29}Si MAS NMR discussed above. The absence of any other observable variation in the local environment of Al within the (N,K)-A-S-H type gel

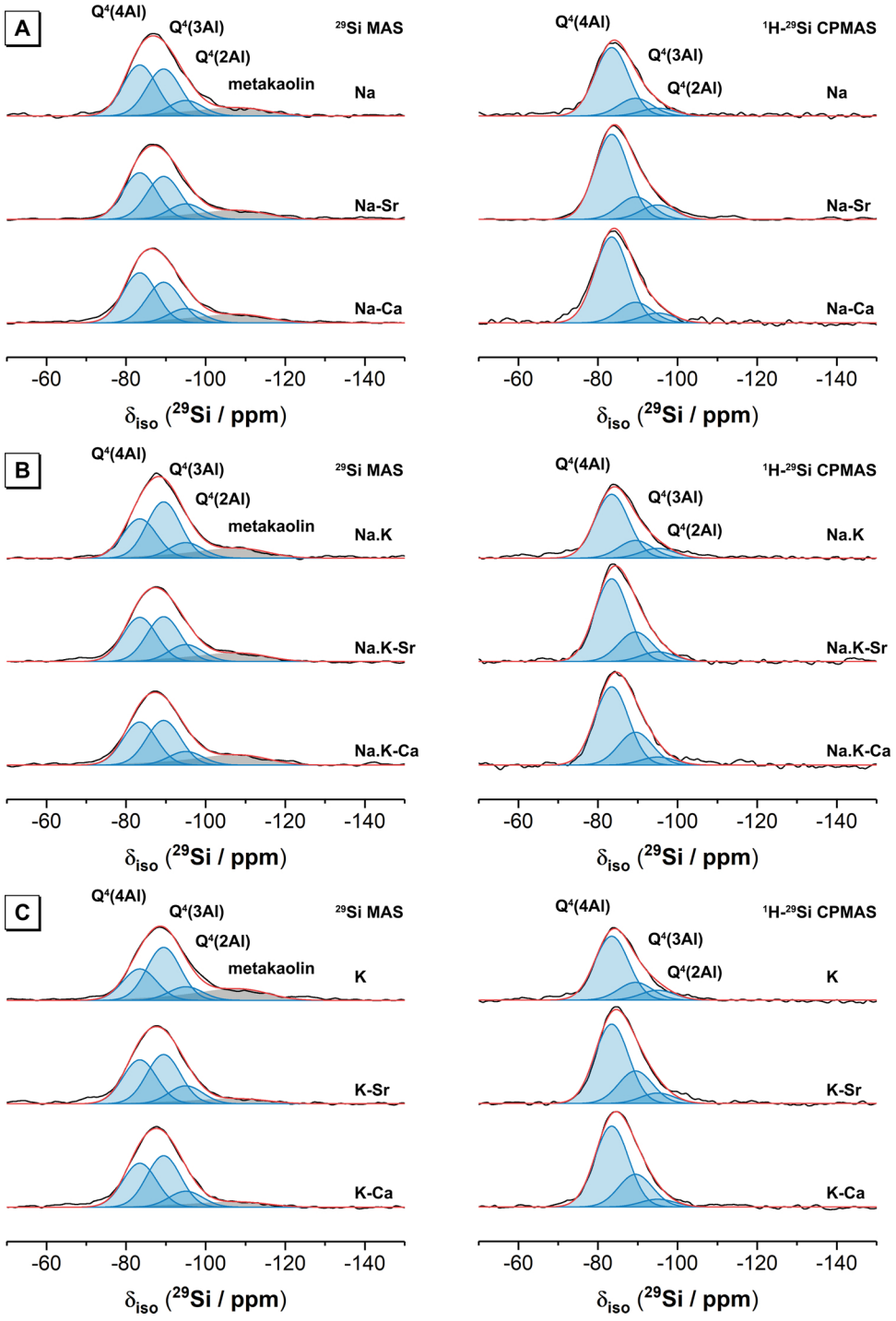

Fig. 4. ^{29}Si MAS (B_0 = 11.7 T, ν_R = 12.5 kHz) NMR and b) ^{1}H-^{29}Si CPMAS (B_0 = 11.7 T, ν_R = 12.5 kHz and Hartmann-Hahn contact period t = 1.7 ms) NMR spectra and associated deconvolutions for geopolymer gels produced by reacting metakaolin with a) sodium silicate, b) a combination of sodium silicate and potassium silicate and c) potassium silicate. In each case, the data are shown in black and the fit (shown in red) is the sum of the deconvoluted peaks. Peaks attributed to Si sites in (N,K)-A-S-H are shown in blue, while those attributed to sites within remnant unreacted metakaolin are shown shaded in grey. (For interpretation of the references to colour in this figure legend, the reader is referred to the web version of this article).

after incorporation of alkaline earth cations indicates that this does not alter the local structure of the gel framework to a significant extent and suggests that the physicochemical properties (e.g. phase stability, durability, ion transport properties) which are controlled, in part, by gel nanostructure are likely to be unaffected.

3.2.3. ^{23}Na MAS NMR

The ^{23}Na MAS NMR spectrum for each geopolymer gel cured at 20 °C (Fig. 4) exhibits a broad resonance spanning from δ_{obs} = 10 to -20 ppm. In geopolymer gels activated with Na_2SiO_3 or a combination of Na_2SiO_3 and K_2SiO_3 this resonance is centred at δ_{obs} = -2.5 ppm and is attributed to Na^+ ions within a (N,K)-A-S-H type gel, charge balancing Al^{3+} ions in fully polymerised q^4 sites (Walkley et al., 2016, 2018; Duxson et al., 2005c). There is no variation in the lineshape and width of the distribution of δ_{obs} between geopolymer gels activated with sodium silicate or with a combination of sodium and potassium silicates, indicating that K^+ is not present the local region surrounding Na^+ ions and therefore suggesting that when present K^+ displaces some of the Na^+ ions and independently charge balances q^4 Al sites without disturbing the electric field gradient surrounding nearby Na^+ ions (likely due to sufficient distance between charge balancing Na^+ and K^+ ions). After incorporation of alkaline earth cations, the ^{23}Na resonance shifts toward lower δ_{obs} values (see inset of Fig. 6), exhibiting a maximum at δ_{obs} = -3.2 ppm in geopolymer gels activated with sodium silicate and δ_{obs} = -3.6 ppm in geopolymer gels activated with a combination of sodium and potassium silicates. This indicates increased shielding of

Table 3
Relative integral areas for $Q^4(4Al)$ and $Q^4(3Al)$ environments within (N,K)-A-S-H in each sample, calculated from the deconvoluted ^{29}Si MAS NMR spectra.

	Relative integral area (%)[a]								
Site	Na	Na-Sr	Na-Ca	NaK	NaK-Sr	NaK-Ca	K	K-Sr	K-Ca
$Q^4(4Al)$	45	44	48	35	42	43	32	40	39
$Q^4(3Al)$	41	41	39	51	42	44	54	44	46
$Q^4(2Al)$	14	15	14	14	16	13	14	16	14
Si/Al	1.21	1.21	1.20	1.24	1.23	1.22	1.26	1.24	1.23

[a] The relative integrated intensity for each resonance is normalised to the sum of all sites within the reaction product and is obtained by simulating the ^{29}Si MAS NMR spectra. Residual unreacted metakaolin component contributions were observed in all geopolymer gel spectra and are shown in Fig. 4 but are excluded from the quantification of (N,K)-A-S-H gel constituents. Estimated error in the relative integral area is 1%. The isotropic chemical shift (δ_{iso}) and the peak full width at half maximum (FWHM) were obtained by simulating the ^{29}Si MAS and ^{1}H-^{29}Si MAS NMR spectra and are δ_{iso} = -84.7 and -89.0 and FWHM = 12.7 and 13.0 for $Q^4(4Al)$ and $Q^4(3Al)$ environments, respectively.

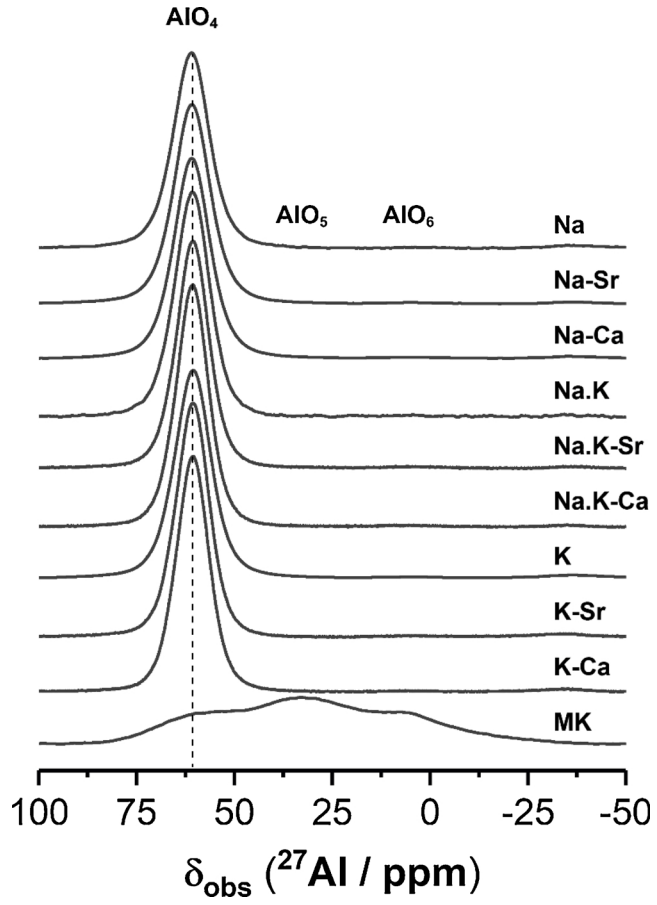

Fig. 5. ^{27}Al MAS NMR spectra (B_0 = 11.7 T, ν_R = 12.5 kHz) for each geopolymer gel, and for metakaolin.

Na^+, consistent with displacement of Na^+ and/or K^+ ions with Sr^{2+} or Ca^{2+} ions, which are expected to fulfil an equivalent charge balancing role. As the charge and ionic size of the alkaline earth and alkali cations differs (Shannon ionic radii 1.02, 1.38, 1.00, and 1.18 Å for octahedrally coordinated Na^+, K^+, Ca^{2+} and Sr^{2+}, respectively), substitution of one double valence alkali earth cation for two single valence alkali cations is expected to result in distortion of the local structure of the (N,K)-A-S-H gel framework. However, the absence of any observable variation in the distribution of δ_{obs} in geopolymer gels after incorporation of Sr^{2+} or Ca^{2+}, regardless of the alkali source, suggests that at the concentrations investigated here both Sr^{2+} and Ca^{2+} are

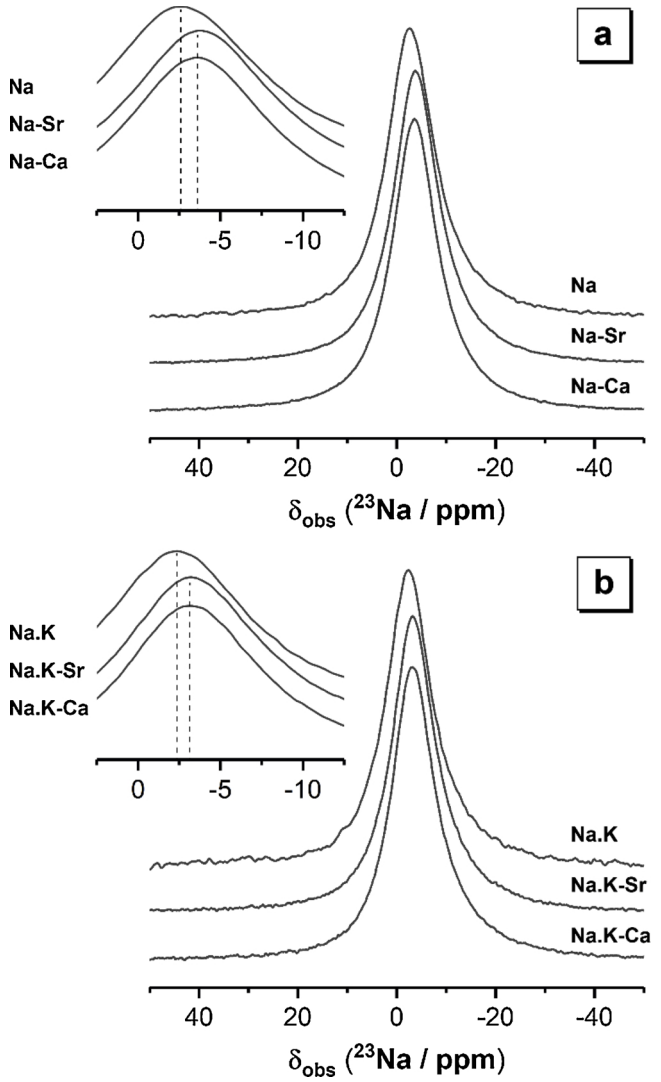

Fig. 6. ^{23}Na MAS NMR spectra (B_0 = 11.7 T, ν_R = 12.5 kHz) for the geopolymer gels produced using solutions of a) sodium silicate and b) mixed sodium-potassium silicate. The inset in each case shows a magnified region of the spectra.

easily accommodated within the (N,K)-A-S-H gel framework. This can be attributed to the high degree of local disorder inherent in these gels which enables significant local variation and distortion in bond angles and lengths (Walkley et al., 2018). Consequently, the physicochemical properties of (N,K)-A-S-H gels that have sorbed different proportions of these alkaline earth cations are likely to be equivalent.

3.3. Fourier transform infrared spectroscopy

FTIR data provide information regarding the energy of bond vibrations that are occurring within the sample (compared with the measurement of atomic nuclei by solid state NMR), and as such can distinguish between Si-O-Si and Si-O-Al bonds and allow observation (albeit indirectly) of the location of non-bridging oxygen sites (Provis and Bernal, 2014) and the presence of ring structures or carbonate species which may not be readily apparent in the solid state NMR data.

The FTIR spectrum for unreacted metakaolin (Fig. 7) exhibits a high intensity band at 1090 cm^{-1} that is assigned to asymmetric stretching of Si–O–T bonds (Hajimohammadi et al., 2011; Lee and van Deventer, 2003; Rees et al., 2007) (where T = Al or Si in tetrahedral coordination), and a low intensity band at 810 cm^{-1} that is assigned to symmetric stretching of Si–O–T bonds (Lee and van Deventer, 2002). The FTIR spectrum for each geopolymer gel cured at 20 °C (Fig. 7) exhibits a

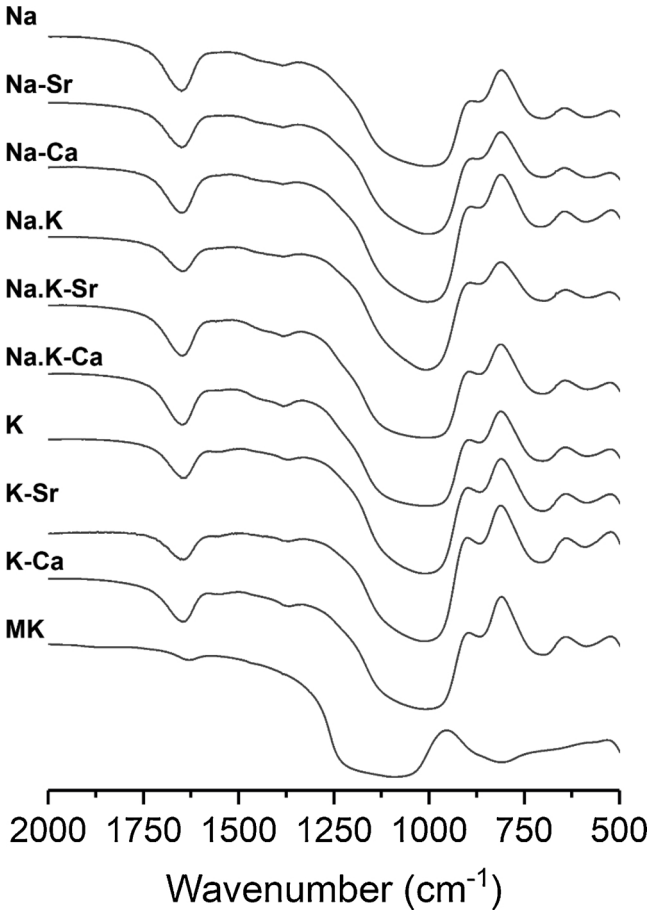

Fig. 7. FTIR spectra of unreacted metakaolin and the geopolymer gels produced using silicate activating solutions as marked on each spectrum.

high intensity band at approximately 1000 cm^{-1} that is also assigned to asymmetric stretching of Si–O–T bonds (Hajimohammadi et al., 2011; Lee and van Deventer, 2003; Rees et al., 2007), with the shift towards lower wavenumbers (compared with the spectrum for unreacted metakaolin) consistent with the formation of an (N,K)–A–S–H gel. This band is relatively broad, and will contain overlapping contributions from both the aforementioned asymmetric Si–O–T stretching band and Si-O-Si bridge vibrations (Criado et al., 2007). The shoulder at approximately 870 cm^{-1} is assigned to the asymmetric stretching of Al–O–Si bonds linking AlO_4 and SiO_4 groups (Farmer, 1974; Gadsden, 1975), while the band at 720 cm^{-1} is assigned to pseudolattice vibrations of small aluminosilicate rings (Handke et al., 1998; Mozgawa, 2001), which have been previously observed in synthetic geopolymer gels (Walkley et al., 2016). A low intensity band at 1650 cm^{-1} is due to the presence of free and chemically bound water, while the small band at 1380 cm^{-1} indicates the presence of a small amount of sodium carbonate in some of the samples (Huang and Kerr, 1960) (not identifiable by XRD). The band at 585 cm^{-1} is assigned to vibrations within 5-membered single rings and 6-membered double rings comprised of TO_4 tetrahedral units (Mozgawa, 2001).

The presence of a shoulder at approximately 1080 cm^{-1} on the main Si-O-T band in these spectra indicates that the geopolymer gels contain some unreacted metakaolin, as identified by ^{29}Si and ^{27}Al MAS NMR and discussed above. There is no significant variation in the main asymmetric Si–O–T stretching band when comparing geopolymer gels produced by reaction of metakaolin with sodium silicate, a combination of sodium silicate and potassium silicate, and potassium silicate. The band assigned to asymmetric stretching of Si–O–T bond becomes broader and shifts towards slightly higher wavenumbers after incorporation of alkaline earth cations. This shift indicates an increase in the fraction of Si-O-Si linkages relative to Si-O-Al linkages in the (N,K)-A-S-H gel, indicating a slight decrease in the gel Al/Si ratio (consistent with ^{29}Si and ^{27}Al MAS NMR data discussed above).

4. Implications for immobilisation of alkaline earth radionuclides

The absence of any (in the case of Al) or minimal (in the case of Si and Na) observable variation in the local environments within the (N,K)-A-S-H type gel after incorporation of non-radioactive isotopes of the alkali earth cations Sr^{2+} (which may be considered as a structural analogue of ^{90}Sr) and Ca^{2+} indicates that this does not significantly alter the local gel structure and suggests that any physicochemical properties (e.g. phase stability, chemical durability, ion sorption properties) that are dictated primarily by the local gel structure are likely to be unaffected. This suggests that metakaolin-based geopolymer gels are excellent candidates for production of wasteforms for immobilisation of radioactive waste containing ^{90}Sr. It also follows that incorporation of alkali or alkaline earth radionuclides of similar ionic size to Sr^{2+} (r = 1.18 Å) such as Ba^{2+} (r = 1.35 Å) and Na^{+} (r = 1.02 Å) can be expected to result in minimal alteration to the local (N,K)-A-S-H gel structure. Even incorporation of radionuclides exhibiting significantly larger ionic sizes such as Cs^{+} (r = 1.67 Å) are unlikely to alter the local gel structure to such an extent as to affect the physicochemical properties of the wasteform (and indeed these may even replace Na^{+} or K^{+} completely (Bell et al., 2009)), as the high extent of local disorder means that the structure can be expected to accommodate significant local variation and distortion in bond angles and lengths. Furthermore, the presence of the partially Sr-substituted zeolite A-Na in these sodium silicate activated metakaolin cements cured at 80 °C will further increase the binding and immobilisation of Sr (Harnett et al., 2019), and suggests that the proto-zeolitic nature of these cements may be exploited to increase the incorporation of alkali or alkaline earth radionuclides of similar ionic size. Future research focusing on leaching of Sr^{2+} and Ca^{2+} from geopolymers, long term phase and structural stability, macroscale engineering properties (e.g. compressive and tensile strength) of geopolymers incorporating Sr^{2+} and Ca^{2+}, and assessment of incorporation of Sr^{2+} and Ca^{2+} in geopolymers above the trace element levels investigated here will be crucial to further assess the viability of these materials for cementation of radioactive waste containing these radionuclides.

5. Conclusions

Multinuclear spectroscopic and diffractometric analysis show that the disordered (N,K)-A-S-H type gel in metakaolin-based geopolymer gels readily accommodates the alkaline earth cations Sr^{2+} and Ca^{2+} into their framework structure. Single pulse ^{29}Si, ^{27}Al and ^{23}Na MAS NMR, and ^{1}H-^{29}Si CP MAS NMR, FTIR spectroscopy and XRD measurements were used to probe nanostructural changes that may result from incorporation of the alkaline earth cations Sr^{2+} and Ca^{2+} in metakaolin-based geopolymer gels, and to investigate the influence of the alkali cations Na^{+} and K^{+} on the alkaline earth incorporation mechanism.

The main reaction product in all geopolymer gels cured at 20 °C was a fully polymerised, X-ray amorphous Al-rich (N,K)-A-S-H type gel, while the zeolitic phases faujasite-Na, and partially Sr-substituted zeolite Na-A were observed as additional phases for geopolymer gels cured at 80 °C. The (N,K)-A-S-H type gel comprises Al and Si in tetrahedral coordination, with Si in $Q^4(4Al)$ and $Q^4(3Al)$ sites, and Na^{+} and K^{+} located within extra-framework sites charge balancing the net negative charge resulting from Al^{3+} in tetrahedral coordination.

Upon incorporation of Sr and Ca, the alkaline earth cations displace some of the alkali cations Na^{+} and K^{+} from the extra-framework sites and fulfil the charge balancing role. The remaining alkali cations are unaffected. Incorporation of alkaline earth cations results in a slight

decrease in the Si/Al ratio of the (N,K)-A-S-H gel due to an increased charge balancing capacity resulting from substitution of divalent alkaline earth cations for monovalent alkali cations. Both Ca and Sr induce the same structural changes and cause a slight decrease in Si/Al ratio in the geopolymer gels. No other changes were observed for geopolymer gels cured at 20 °C, however in those cured at 80 °C incorporation of Sr appeared to promote the formation of LTA (zeolite A) over FAU (faujasite) zeolite phases.

The findings presented here have significant implications for the long term stability and durability of these materials and suggests that metakaolin-based geopolymer gels are excellent candidates for production of wasteforms for immobilisation of radioactive waste containing ^{90}Sr.

Acknowledgements

This work has been funded by the Engineering and Physical Sciences Research Council (EPSRC), UK, through grant EP/P013171/1. We wish to thank and acknowledge Dr Sandra van Meurs, Department of Chemistry, The University of Sheffield, for assistance in acquiring the NMR data and insightful discussions related to this work. We are also very grateful to the PQ Corporation for the provision of alkali silicate solutions for this experimental programme.

References

Aldridge, L., Day, R., Leung, S., Ray, A., Stevens, M., Knight, R., Mapson, C., 1997. Cs retention in zeolites immobilised by portland cement. In: Proceedings of the Materials Research Society's Symposium on Mechanisms of Chemical Degradation of Cement-Based Systems. E&FN Spon, London. pp. 358–365.

Arbel Haddad, M., Ofer-Rozovsky, E., Bar-Nes, G., Borojovich, E.J.C., Nikolski, A., Mogiliansky, D., Katz, A., 2017. Formation of zeolites in metakaolin-based geopolymers and their potential application for Cs immobilization. J. Nucl. Mater. 493, 168–179.

Barrer, R.M., Mainwaring, D.E., 1972a. Chemistry of soil minerals. Part XIII. Reactions of metakaolinite with single and mixed bases. J. Chem. Soc. Dalton Trans. 2534–2546.

Barrer, R.M., Mainwaring, D.E., 1972b. Chemistry of soil minerals. Part XI. Hydrothermal transformations of metakaolinite in potassium hydroxide. J. Chem. Soc. Dalton Trans. 1254–1259.

Barrer, R.M., Cole, J.F., Sticher, H., 1968. Chemistry of soil minerals. Part V. Low temperature hydrothermal transformations of kaolinite. J. Chem. Soc. A 2475–2485.

Bell, J.L., Driemeyer, P.E., Kriven, W.M., 2009. Formation of ceramics from metakaolin-based geopolymers: part I—Cs-based geopolymer. J. Am. Ceram. Soc. 92, 1–8.

Bernal, S.A., Provis, J.L., Walkley, B., San Nicolas, R., Gehman, J.D., Brice, D.G., Kilcullen, A.R., Duxson, P., van Deventer, J.S.J., 2013. Gel nanostructure in alkali-activated binders based on slag and fly ash, and effects of accelerated carbonation. Cem. Concr. Res. 53, 127–144.

Boden, S.C., 2002. Nirex Vault Environment Feasibility Study: Summary Report. NNC Ltd.

Catalfamo, P., Di Pasquale, S., Corigliano, F., Mavilia, L., 1997. Influence of the calcium content on the coal fly ash features in some innovative applications. Resour. Conserv. Recycl. 20, 119–125.

Criado, M., Fernández-Jiménez, A., Palomo, A., 2007. Alkali activation of fly ash: effect of the SiO_2/Na_2O ratio: part I: FTIR study. Microporous Mesoporous Mater. 106, 180–191.

Criado, M., Fernández-Jiménez, A., Palomo, A., Sobrados, I., Sanz, J., 2008. Effect of the SiO_2/Na_2O ratio on the alkali activation of fly ash. Part II: ^{29}Si MAS-NMR survey. Microporous Mesoporous Mater. 109, 525–534.

Davis, M.E., Lobo, R.F., 1992. Zeolite and molecular sieve synthesis. Chem. Mater. 4, 756–768.

Duxson, P., Lukey, G.C., Separovic, F., van Deventer, J.S.J., 2005c. Effect of alkali cations on aluminum incorporation in geopolymeric gels. Ind. Eng. Chem. Res. 44, 832–839.

Duxson, P., Provis, J.L., Lukey, G.C., Separovic, F., van Deventer, J.S.J., 2005a. ^{29}Si NMR study of structural ordering in aluminosilicate geopolymer gels. Langmuir 21, 3028–3036.

Duxson, P., Provis, J.L., Lukey, G.C., Separovic, F., van Deventer, J.S.J., 2005b. ^{29}Si NMR study of structural ordering in aluminosilicate geopolymer gels. Langmuir 21, 3028–3036.

Duxson, P., Lukey, G.C., van Deventer, J.S.J., 2006. Evolution of gel structure during thermal processing of Na-geopolymer gels. Langmuir 22, 8750–8757.

Engelhardt, G., Lohse, U., Lippmaa, E., Tarmak, M., Mägi, M., 1981. ^{29}Si-NMR-Untersuchungen zur Verteilung der Silicium-und Aluminiumatome im Alumosilicatgitter von Zeolithen mit Faujasit-Struktur. Z. Anorg. Allg. Chemie 482, 49–64.

Farmer, V.C., 1974. The Infrared Spectra of Minerals. Mineralogical Society, London.

Felmy, A.R., Mason, M.J., Gassman, P.L., McCready, D.E., 2003. The formation of Sr silicates at low temperature and the solubility product of tobermorite-like $Sr_5Si_6O_{16}(OH)_2.5H_2O$. Am. Mineral. 88, 73–79.

Fernández-Jiménez, A., Palomo, A., Sobrados, I., Sanz, J., 2006. The role played by the reactive alumina content in the alkaline activation of fly ashes. Microporous Mesoporous Mater. 91, 111–119.

Gadsden, J.A., 1975. Infrared Spectra of Minerals and Related Inorganic Compounds. Butterworths, London.

Gaona, X., Kulik, D.A., Macé, N., Wieland, E., 2012. Aqueous–solid solution thermodynamic model of U(VI) uptake in C–S–H phases. Appl. Geochem. 27, 81–95.

Goñi, S., Guerrero, A., Lorenzo, M.P., 2006. Efficiency of fly ash belite cement and zeolite matrices for immobilizing cesium. J. Hazard. Mater. 137, 1608–1617.

Godfrey, H., Cann, G., 2015. Effect of Chloride on Magnox Corrosion With Respect to Carbon-14 Release Post Closure. NNL, Risley.

Hajimohammadi, A., Provis, J.L., van Deventer, J.S.J., 2010. Effect of alumina release rate on the mechanism of geopolymer gel formation. Chem. Mater. 22, 5199–5208.

Hajimohammadi, A., Provis, J.L., van Deventer, J.S.J., 2011. The effect of silica availability on the mechanism of geopolymerisation. Cem. Concr. Res. 41, 210–216.

Handke, M., Sitarz, M., Mozgawa, W., 1998. Model of silicooxygen ring vibrations. J. Mol. Struct. 450, 229–238.

Harnett, L.C., Gardner, L.J., Sun, S.-K., Mann, C., Hyatt, N.C., 2019. Reactive spark plasma sintering of Cs-exchanged chabazite: characterisation and durability assessment for Fukushima Daiichi NPP clean-up. J. Nucl. Sci. Technol. https://doi.org/10.1080/00223131.2019.1602484. in press.

Huang, C.K., Kerr, P.F., 1960. Infrared study of the carbonate minerals. Am. Mineral. 45, 311.

Hunter, F., Swift, B., 2013. An Assessment of the Generation of GDF-derived Gas Using the 2007 Derived Inventory. AMEC.

Ismail, I., Bernal, S.A., Provis, J.L., Hamdan, S., van Deventer, J.S.J., 2013. Drying-induced changes in the structure of alkali-activated pastes. J. Mater. Sci. 48, 3566–3577.

Jacobs, P.A., 1992. Some thermodynamic and kinetic effects related to zeolite crystallization. In: Derouane, E.G., Lemos, F., Naccache, C., Ribeiro, F.R. (Eds.), Zeolite Microporous Solids: Synthesis, Structure, and Reactivity, Springer. Dordrecht, Netherlands, pp. 3–18.

Kirishima, A., Sasaki, T., Sato, N., 2015. Solution chemistry study of radioactive Sr on Fukushima Daiichi NPS site. J. Nucl. Sci. Technol. 52, 152–161.

Kobera, L., Brus, J., Klein, P., Dedecek, J., Urbanova, M., 2014. Biaxial Q-shearing of ^{27}Al 3QMAS NMR spectra: Insight into the structural disorder of framework aluminosilicates. Solid State Nucl. Magn. Reson. 57–58, 29–38.

Kolodziejski, W., Klinowski, J., 2002. Kinetics of cross-polarization in solid-state NMR: a guide for chemists. Chem. Rev. 102, 613–628.

Koma, Y., Shibata, A., Ashida, T., 2017. Radioactive contamination of several materials following the Fukushima Daiichi Nuclear Power Station accident. Nucl. Mater. Energy 10, 35–41.

Kowalczyk, G., Roberts, J.E., 1994. Solid State ^{29}Si NMR determination of crystalline silica in natural iron oxide pigments. Anal. Chim. Acta 286, 25–35.

Kuenzel, C., Cisneros, J.F., Neville, T.P., Vandeperre, L.J., Simons, S.J.R., Bensted, J., Cheeseman, C.R., 2015. Encapsulation of Cs/Sr contaminated clinoptilolite in geopolymers produced from metakaolin. J. Nucl. Mater. 466, 94–99.

Lausen, S.K., Lindgreen, H., Jakobsen, H.J., Nielsen, N.C., 1999. Solid-state ^{29}Si MAS NMR studies of illite and illite-smectite from shale. Am. Mineral. 84, 1433–1438.

Lecomte, I., Henrist, C., Liégeois, M., Maseri, F., Rulmont, A., Cloots, R., 2006. (Micro)-structural comparison between geopolymers, alkali-activated slag cement and Portland cement. J. Eur. Ceram. Soc. 26, 3789–3797.

Lee, W.K.W., van Deventer, J.S.J., 2002. The effects of inorganic salt contamination on the strength and durability of geopolymers. Colloids Surfaces A – Physicochem. Eng. Aspects 211, 115–126.

Lee, W.K.W., van Deventer, J.S.J., 2003. Use of infrared spectroscopy to study geopolymerization of heterogeneous amorphous aluminosilicates. Langmuir 19, 8726–8734.

Mandaliev, P., Dähn, R., Tits, J., Wehrli, B., Wieland, E., 2010. EXAFS study of Nd(III) uptake by amorphous calcium silicate hydrates (C–S–H). J. Colloid Interface Sci. 342, 1–7.

Massiot, D., Fayon, F., Capron, M., King, I., Le Calvé, S., Alonso, B., Durand, J.-O., Bujoli, B., Gan, Z., Hoatson, G., 2002. Modelling one- and two-dimensional solid-state NMR spectra. Magn. Reson. Chem. 40, 70–76.

McCormick, A., Bell, A.T., 1989. The solution chemistry of zeolite precursors. Catalysis Rev. Sci. Eng. 31, 97–127.

Mozgawa, W., 2001. The relation between structure and vibrational spectra of natural zeolites. J. Mol. Struct. 596, 129–137.

Munthali, M.W., Johan, E., Aono, H., Matsue, N., 2015. Cs^+ and Sr^{2+} adsorption selectivity of zeolites in relation to radioactive decontamination. J. Asian Ceram. Soc. 3, 245–250.

Myers, S., Cygan, R., Assink, R., Boslough, M., 1998. ^{29}Si MAS NMR relaxation study of shocked Coconino sandstone from Meteor Crater, Arizona. Phys. Chem. Miner. 25, 313–317.

Nuclear Decommissioning Authority, 2014. Geological Disposal: Guidance on the Application of the Waste Package Specifications for Unshielded Waste Packages. Oxford.

Ochs, M., Mallants, D., Wang, L., 2015. Radionuclide and Metal Sorption on Cement and Concrete. Springer International Publishing, Switzerland.

Ofer-Rozovsky, E., Arbel Haddad, M., Bar-Nes, G., Borojovich, E.J.C., Binyamini, A., Nikolski, A., Katz, A., 2019. Cesium immobilization in nitrate-bearing metakaolin-based geopolymers. J. Nucl. Mater. 514, 247–254.

Perera, D.S., Vance, E.R., Aly, Z., Davis, J., Nicholson, C.L., 2006. Immobilization of Cs and Sr in geopolymers with Si/Al molar ratio of ~ 2. Ceram. Trans. 176, 91–96.

Phair, J.W., Smith, J.D., Van Deventer, J.S.J., 2003. Characteristics of aluminosilicate hydrogels related to commercial "geopolymers". Mater. Lett. 57, 4356–4367.

Prentice, D.P., Walkley, B., Bernal, S.A., Bankhead, M., Hayes, M., Provis, J.L., 2019. Thermodynamic modelling of BFS-PC cements under temperature conditions relevant

to the geological disposal of nuclear wastes. Cem. Concr. Res. 119, 21–35.
Provis, J.L., Bernal, S.A., 2014. Geopolymers and related alkali-activated materials. Annu. Rev. Mater. Res. 44, 299–327.
Provis, J.L., Duxson, P., Lukey, G.C., van Deventer, J.S.J., 2005a. Statistical thermodynamic model for Si/Al ordering in amorphous aluminosilicates. Chem. Mater. 17, 2976–2986.
Provis, J.L., Lukey, G.C., van Deventer, J.S.J., 2005b. Do geopolymers actually contain nanocrystalline zeolites? A reexamination of existing results. Chem. Mater. 17, 3075–3085.
Provis, J.L., Walls, P.A., van Deventer, J.S.J., 2008. Geopolymerisation kinetics. 3. Effects of Cs and Sr salts. Chem. Eng. Sci. 63, 4480–4489.
Provis, J.L., Palomo, A., Shi, C.J., 2015. Advances in understanding alkali-activated materials. Cem. Concr. Res. 78, 110–125.
Qian, G., Li, Y., Yi, F., Shi, R., 2002. Improvement of metakaolin on radioactive Sr and Cs immobilization of alkali-activated slag matrix. J. Hazard. Mater. 92, 289–300.
Rees, C.A., Provis, J.L., Lukey, G.C., van Deventer, J.S.J., 2007. Attenuated total reflectance Fourier transform infrared analysis of fly ash geopolymer gel aging. Langmuir 23, 8170–8179.
Rickard, W.D.A., Williams, R., Temuujin, J., van Riessen, A., 2011. Assessing the suitability of three Australian fly ashes as an aluminosilicate source for geopolymers in high temperature applications. Mater. Sci. Eng. A 528, 3390–3397.
Rickard, W.D.A., Kealley, C.S., van Riessen, A., 2015. Thermally induced microstructural changes in fly ash geopolymers: experimental results and proposed model. J. Am. Ceram. Soc. 98, 929–939.
Rivera, O.G., Long, W.R., Weiss Jr., C.A., Moser, R.D., Williams, B.A., Torres-Cancel, K., Gore, E.R., Allison, P.G., 2016. Effect of elevated temperature on alkali-activated geopolymeric binders compared to portland cement-based binders. Cem. Concr. Res. 90, 43–51.
Shannon, R., 1976. Revised effective ionic radii and systematic studies of interatomic distances in halides and chalcogenides. Acta Crystallogr. Section A 32, 751–767.
Stebbins, J.F., Kroeker, S., Lee, S.K., Kiczenski, T.J., 2000. Quantification of five- and six-coordinated aluminum ions in aluminosilicate and fluoride-containing glasses by high-field, high-resolution ^{27}Al NMR. J. Non-Cryst. Solids 275, 1–6.
Tits, J., Wieland, E., Müller, C.J., Landesman, C., Bradbury, M.H., 2006. Strontium binding by calcium silicate hydrates. J. Colloid Interface Sci. 300, 78–87.
Tits, J., Walther, C., Stumpf, T., Macé, N., Wieland, E., 2015. A luminescence line-narrowing spectroscopic study of the uranium(VI) interaction with cementitious materials and titanium dioxide. Dalton Trans. 44, 966–976.
Tusa, E., 2014. Cesium and strontium removal with highly selective ion exchange media in Fukushima and cesium removal with less selective media. In: Proceedings of the Waste Management Symposia. Phoenix, Arizona, USA. #14018.
Vandevenne, N., Iacobescu, R.I., Carleer, R., Samyn, P., D'Haen, J., Pontikes, Y., Schreurs, S., Schroeyers, W., 2018. Alkali-activated materials for radionuclide immobilisation and the effect of precursor composition on Cs/Sr retention. J. Nucl. Mater. 510, 575–584.
Vespa, M., Dähn, R., Wieland, E., 2014. Competition behaviour of metal uptake in cementitious systems: An XRD and EXAFS investigation of Nd- and Zn-loaded 11Å tobermorite. Phys. Chem. Earth Parts A/B/C 70–71, 32–38.
Walkley, B., San Nicolas, R., Sani, M.A., Gehman, J.D., van Deventer, J.S.J., Provis, J.L., 2016. Phase evolution of Na_2O-Al_2O_3-SiO_2-H_2O gels in synthetic aluminosilicate binders. Dalton Trans. 45, 5521–5535.
Walkley, B., Rees, G.J., San Nicolas, R., van Deventer, J.S.J., Hanna, J.V., Provis, J.L., 2018. New structural model of hydrous sodium aluminosilicate gels and the role of charge-balancing extra-framework Al. J. Phys. Chem. C 122, 5673–5685.
Wieland, E., Tits, J., Kunz, D., Dähn, R., 2008. Strontium uptake by cementitious materials. Environ. Sci. Technol. 42, 403–409.
Williams, B.D., Neeway, J.J., Snyder, M.M.V., Bowden, M.E., Amonette, J.E., Arey, B.W., Pierce, E.M., Brown, C.F., Qafoku, N.P., 2016. Mineral assemblage transformation of a metakaolin-based waste form after geopolymer encapsulation. J. Nucl. Mater. 473, 320–332.
Blackford, M.G., Hanna, J.V., Pike, K.J., Vance, E.R., Perera, D.S., 2007. Transmission electron microscopy and nuclear magnetic resonance studies of geopolymers for radioactive waste immobilization. J. Am. Ceram. Soc. 90, 1193–1199.
van Jaarsveld, J.G.S., van Deventer, J.S.J., 1999. Effect of the alkali metal activator on the properties of fly ash-based geopolymers. Ind. Eng. Chem. Res. 38, 3932–3941.